GNITED MINDS
Journals

Journal of Advances in Science and Technology

Vol. V, Issue No. X, August-2013, ISSN 2230-9659

A COMPARATIVE RESEARCH ON GENERATION OF SILK SERICIN/SILK FIBROIN COMBINE NANOFIBERS

www.ignited.in

Journal of Advances in Science and Technology
Vol. V, Issue No. X, August-2013, ISSN 2230-9659

A Comparative Research on Generation of Silk Sericin/Silk Fibroin Combine Nanofibers

Deepti[1]* Akhilesh Kumar[2]

[1]Research Scholar, Magadh University, Department of Zoology, A.N. College, Patna

[2]Asst. Professor, Department of Zoology, A. N. College, Patna

Abstract – Silk sericin (SS)/silk fibroin (SF) blend nanofibers have been generated by electrospinning in a binary SS/SF trifluoroacetic harsh corrosive (TFA) solution framework, which was ready by blending 20 wt.% SS TFA solution and 10 wt.% SF TFA solution to give distinctive pieces. The diameters of the SS/SF nanofibers extended from 33 to 837 nm, and they demonstrated a round cross segment. The surface of the SS/SF nanofibers was smooth, and the fibers controlled a dab free structure. The normal diameters of the SS/SF (75/25, 50/50, and 25/75) blend nanofibers were much thicker than that of SS and SF nanofibers. The SS/SF (100/0, 75/25, and 50/50) blend nanofibers were effectively dissolved in water, while the SS/SF (25/75 and 0/100) blend nanofibers couldn't be totally dissolved in water. The SS/SF blend nanofibers couldn't be totally dissolved in methanol. The SS/SF blend nanofibers were portrayed by Fourier change infrared (FTIR) spectroscopy, differential filtering calorimetry, and differential thermal analysis. FTIR indicated that the SS/SF blend nanofibers controlled an irregular curl conformity and K-sheet structure.

◆

INTRODUCTION

Electrospinning is an intriguing and successful process for generating nanoscale fibers with diameters in the nanometer to micrometer extent. These nanofibers have high purpose, high particular surface range, and high porosity with quite little pore size . In this way, the micro/nanofibers can reenact the extracellular framework and improve cell movement and burgeoning. They are connected in the biomedical area for drug conveyance, wound dressing, tissue engineering platforms, and different utilization.

Silk cocoon filaments from the Bombyx mori silkworm are made out of SS and SF. SS is bio-orchestrated exclusively in the center silk organ and is around the range of 25-30% of silk fiber mass. Sericin layers fibroin strings to paste them together and fills the crevices to upgrade the toughness of the cocoon fiber . Sericin is made out of an expansive number of hydrophilic amino acids, for example, serine, glycine, lysine, and so on. Sericin is an essential bio-material, which could be utilized within the restorative and corrective fields, since it shows exceptional similarity to human tissues, biodegradation and oxidation safety, antibacterial properties, and UV safety. Moreover, sericin ingests and discharges moisture promptly and shows the inhibitory movement of tyrosine and kinase, and is utilized broadly as a part of restorative provisions. SF has been broadly utilized within tissue engineering due to particular useful properties, incorporating great biocompatibility, exceptional oxygen and water vapor penetrability, and biodegradabil- ity. There are substantial amounts of productions on SF and Sf/polymer blend nanofibers, however there are not many distributions on the SS/SF blend nanofibers.

In this study, we present a novel approach to plan SS/SF nanofibers. Our effects show the fruitful preparation of SS/SF blend nanofibers with smooth surfaces by means of electrospinning from SS/SF blend solutions, and we investigate their atomic compliance and physical properties.

EXPERIMENT

Materials : Sericin as the powder form of silk sericin (SS) was purchased from Wako Pure Chemical Industries, Ltd. (3-12, Chuoh-ku, Osaka city, 540-8605, Japan) (Lot. CDR4258). Silk fibroin (SF) film was prepared by casting 2 wt.% SF solution in flat-bottomed polystyrene dishes at room temperature in a flow cabinet. SF solution was prepared by dissolving SF fibers in 8 M LiBr solution at 60°C for 30 min and then dialyzed against water at 5°C for 4 days using cellulose dialysis tubes.

Preparation of the SS/SF blended solution : SS solution (20 wt.%) and SF solution (10 wt.%) were prepared by stirring the samples in trifluoroacetic acid (TFA) at 25°C for 3 h. Solutions of 0.45, 0.3, and 0.15 g SS were mixed with 0.3, 0.6, and 0.9 g SF solutions, respectively, so that the SS/SF (w/w:

75/25, 50/50, and 25/75) blend solutions were prepared. The SS/SF (75/ 25) blend nanofibers were produced from solutions containing 75 wt.% SS and 25 wt.% SF. The pure and mixed solutions were stirred for 3 h. These sample solutions were stored in the refrigerator (4°C) for 12 h, while the electrospinning solution was prepared. The sample nanofibers were produced by electrospinning the SS/SF solutions, having different sample compositions (SS/SF: 100/0, 75/25, 50/50, 25/75, and 0/100).

Electrospinning setup and process : Electrospinning of the solutions was conducted under normal atmospheric conditions. The electrospinning apparatus consisted of a syringe (SS-01T, Terumo Corporation, Tokyo, Japan), needle (NN-2238N, Terumo Corporation), aluminum collecting screen, and syringe pump. The spinning speed of the syringe pump was adjusted within the range 0.003-0.320 cm/min. High voltage power (Kato Tech Company, Tokyo, Japan), 26, Nishi 9-jou, Minami-ku, Kyoto city, 601-8447, Japan) was supplied in the range 0 to 40 kV. The sample solution was placed into the 1-ml syringe, with a 21- gauge needle (inner diameter 0.3 mm). The voltage was applied between the end of the needle and collecting screen. Nanofiber mats were produced on the aluminum collecting screen. The electrospinning was conducted with values of working distance, applied voltage, and flow rate at 15 cm, 25 kV, and 0.06 cm/ min, respectively.

Characterization : The morphology and the diameter of nanofibers were determined with a scanning electron microscope (SEM) (S-3000N, Hitachi, 1-6-6, Marunouchi, Chiyoda-ku, Tokyo, 100-8280, Japan. For SEM measurements, samples were placed on an aluminum circular plate and coated with a gold layer. The mean diameter and distribution were obtained using the commercial software package, SPSS. Fourier transform infrared (FT-IR) spectroscopy was measured with a Shimadzu FT-IR-8400S infrared spectrometer (Shimadzu corporation, 1, Kuwabara-machi, Chuoh-ku, Kyoto City, 604-8511, Japan) by the ATR method in the region of 1800-700 cm^{-1} at room temperature. The spectra of samples were acquired in transmittance mode with a resolution of 4 cm^{-1} and spectral range of 4,000-500 cm^{-1}. Infrared spectra were recorded from 16 scans per sample.

Differential scanning calorimetry (DSC) curves of samples were measured with a DSC instrument (Thermo Plus DSC 8230, Rigaku Corporation, Tokyo, Japan) under normal atmospheric conditions, at a heating rate of 10°C/min. The temperature ranged from room temperature to 300°C, and the sample weight was 3 mg. Differential thermal analysis (DTA) measurements were carried out using a DTA instrument (Thermo Plus TG 8120, Rigaku Corporation) under a nitrogen atmosphere in the range from room temperature to 300°C and at a heating rate of 10°C/min. The sample weight was 6 mg.

RESULTS AND DISCUSSION

SEM images and diameter dispersion of the SS/SF blend nanofibers : Figure 1 shows the SS/SF nanofibers and their comparing diameter appropriations for the distinctive degrees of SS/SF. "As-spun" nanofibers displayed smooth surfaces, round cross areas, and dab free structures. The diameters ran between 33 and 837 nm. The normal diameters of the SS/SF blend nanofibers in Figure 1a,b,c,d,e were 156, 242, 221, 172, and 160 nm, separately. The normal diameters of the SS/SF (75/25, 50/50, and 25/75) blend nanofibers were thicker than SS (100/0) and SF (0/100) nanofibers. The normal diameters of SS/SF blend nanofibers (Figure 1b,c,d) diminished with an expanding measure of the SF part.

Impact of dissolution time : We planned blend solutions by the accompanying systems. The SS/SF blend solution was firstly blended at 25° C for 6 h, then saved in the refrigerator (4°c) for 12 h, and mixed again at 25°c for 222 h (10 days aggregate). Promptly in the wake of blending, specimen nanofibers were pro¬duced by electrospinning.

Figure 2 demonstrated the SEM micrographs and diameter dispersion outlines of the SS, SS/SF (50/50), and SF nanofibers. SS nanofibers (Figure 2a) obtained by electrospinning with SS solution, having a dissolving time of 10 days, showed dab free and astounding nanofibers. The SS/SF (50/50) and SF nanofibers indicated smooth nanofibers holding some round and shaft like globules. The amount of dabs in the SF nanofi- bers (Figure 2c) was significantly more than that in the SS/SF (50/50) (Figure 2b) blend nanofibers.

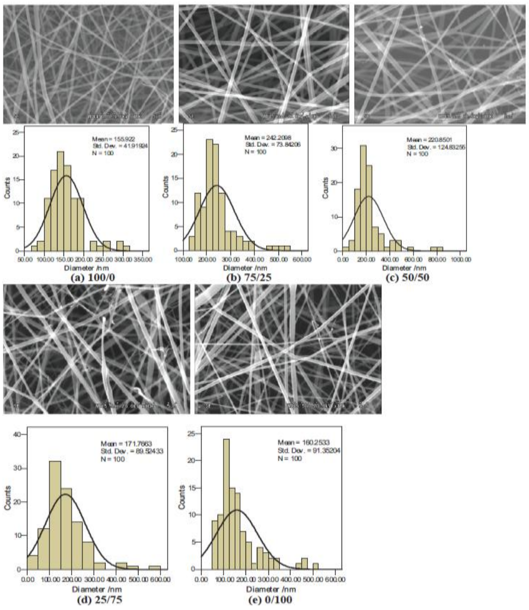

Figure 1 SEM micrographs and diameter distributions of the SS/SF blend nanofibers. SS/SF (w/w): (a) 100/0, (b) 75/25, (c) 50/50, (d) 25/75, (e) 0/100.

It is of vital to note that the normal diameter of nanofibers (100/0) is something like 155 nm (Figure 1a), though being 211 nm in Figure 2a. This slight inconsistency is most likely because of the dissolving conditions, incorporating dissolving temperature and time of the nanofibers. The dissolving temperature and time of SS/SF 100/0 (Figure 1a) are 25°c and 3 h, individually, while dissolving temperature and time for the nanofibers from SS/SF 100/0 (Figure 2a) are 25°c and 10 days. We further research the impact of the dissolving conditions on diameter dissemination of nanofibers. The normal diameters of the SS/SF blend nanofibers (Figure 2a,b,c) were 211, 119, and 83 nm. The normal diameters of these SS/SF nano- fibers diminished with expanding SF substance.

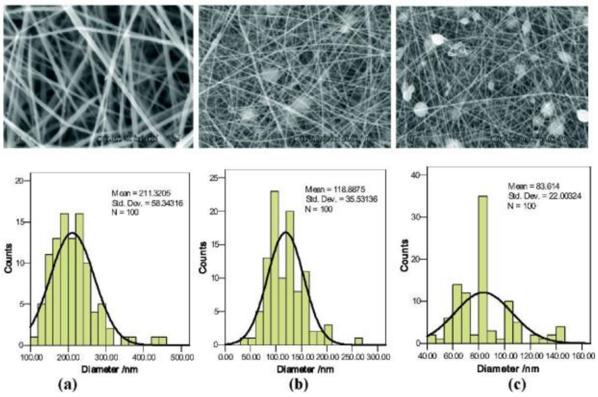

(a) (b) (c)

Figure 2 SEM micrographs and diameter distributions of the SS/SF (50/50) blend nanofibers. In relation to the dissolving time. Dissolving time and SS/SF (w/w): (a) 10 days, 100/0, (b) 10 days, 50/50, (c) 10 days, 0/100.

Solvency of the SS/SF blend nanofibers : We inspected the dissolvability of the SS/SF blend nanofibers in water and in methanol. The SS nanofibers were totally dissolved in water after a short drenching time (1 h), while the SF nanofibers were not dissolved in water. The SS/SF blend nanofibers, holding higher measures of SS, were all the more effectively dissolved in water. The SS/SF (100/0, 75/25, and 50/50) blend nanofibers were totally dissolved in water inside 1 h. Then again, when the SF segment was more excellent than the SS part, as in the SS/SF blend nanofibers (25/75), they couldn't be totally dissolved in water. Over the same time period, the SS/SF blend nanofibers couldn't be dissolved in methanol.

FTIR spectra : FTIR spectroscopy is an influential system for contemplating structure at the sub-atomic level. FTIR shows the particular absorption groups delicate to the atomic conformity of silk proteins. The spectra of SS and the SS/ SF blend nanofibers (Figure 3a,b,c,d,e,f) were character¬ized by the absorption groups at 1,641, 1,647, 1,645, 1,645, 1,643, and 1,643 cm^{-1}, which were ascribed to the arbitrary curl compliance. SF indicated at 1,625 cm^{-1} (amide I), and the SS/SF nanofibers demonstrated absorption tops at around 1,512 cm^{-1} (amide II), ascribed to the fi-sheet compliance. Amide III indicated in SS and SF at 1,238 and 1,233 cm^{-1} attributable to fi-sheet structure, while the absorption groups of amide III of the SS/SF (50/50, 25/75, and 0/100) blend nanofibers (Figure 3d,e, f) demonstrated quite little shoulder crests. In the meantime, amide III vanished in the SS/SF (100/0 and 25/75) blend nanofibers' spectra (Figure 3b,c). It is worth noting that a shoulder absorption band at 1,218 cm^{-1} exists in the TFA range (not indicated in Figure 3). The sub-atomic compliance of the SS/SF blend nanofibers are made out of an arbitrary loop and fi-sheet structure (Figure 3).

The IR spectra of the SS/SF blend nanofibers (Figure 3b,c,d,e,f) were similar to each other. The minor absorption band at 1,787 cm^{-1} did not appear in the SS or SF samples (Figure 3a,h). According to FTIR spectra of TFA, performed by FTIR analysis equipped with an ATR (attenuated total reflectance) accessory and ZnSe crystal, the absorption at 1,787 cm^{-1} is specifically observed (unpublished data). However, according to Figure 3, it is difficult to observe this peak for curves d and f. It seems that absorption band at 1,787 cm^{-1} is due to the trace amount of TFA contained in the SS/SF blend

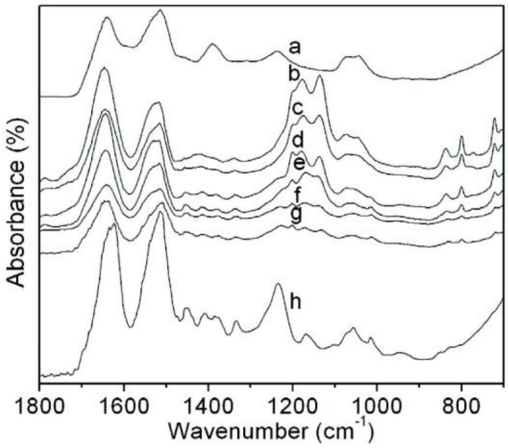

Figure 3 FTIR spectra of SS, SS/SF blend nanofibers, heated SS/SF (50/50) blend nanofibers, and SF. Sample: a, powder form of silk sericin; b, c, d, e, f, SS/SF blend nanofibers with different compositions (100/0, 75/25, 50/50, 25/75, 0/100); g SS/SF blend nanofiber (50/50), heat- treated at 160°C for 30 min; h SF film nanofibers and that the molecular interaction between the trace amount of TFA and SS is slightly stronger than that between TFA and SF.

It was of investment to note that this absorption band was located in the SS/SF blend nanofibers (Figure 3b,c, d,e,f). The SS/SF (50/50, 25/75, and 0/100) blend nanofibers (Figure 3d,e,f) and SF (Figure 3h) controlled a minor absorption band at 1,454 cm^{-1}. The SS/SF blend nanofibers and SF demonstrated powerless absorption groups at 1,408 and 1,334 cm^{-1}. SS showed an unique absorption band at 1,390 cm^{-1}, and SF demonstrated a feeble crest at 1,386 cm^{-1}. Be that as it may, this top had vanished in the SS/SF (100/0 and 75/25) blend nanofibers' spectra (Figure 3b,c). Around 1,200 cm^{-1}, there was a feeble crest displayed in the spectra of the SS/SF blend nanofibers with the exception of SS nanofibers. The SF (Figure 3h) indicated frail absorption groups at 1,168 and 1,100 cm^{-1}. All SS/ SF blend nanofibers (Figure 3b,c,d,e,f) had the absorption groups around 1,170 and 1,136 cm^{-1}. SS nanofibers controlled absorption groups around 1,072 and 1,047 cm- \ while SF nanofibers showed at around 1,014 cm^{-1}.

For these absorption groups, the SS/SF blend nanofibers indicated absorption band attributes of both SS and SF pure segments covering in the relating absorption locale. The SS/SF blend nanofibers indicated absorption groups at 837, 801, and 720 cm^{-1}. Then again, SS and SF completed not have these absorption groups. The power of these absorption groups expanded with expanding SS substance. The power of the FTIR range of SS/SF (50/50) blend nanofibers, hotness treated at 160°c for 30 min demonstrated in Figure 3g, got minor contrasted and those of the SS/SF (50/50) nanofi- bers (Figure 3d).

CONCLUSIONS

We succeeded in processing SS/SF blend nanofibers by electrospinning with a SS/SF TFA blend solution. The "as-spun" nanofibers showed smooth surfaces, round cross segments, and dot free structures. The normal diameters of SS/SF (75/25, 50/50, and 25/75) blend nanofibers were thicker than those of SS or SF nanofi- bers. The mean diameter of these blended nanofibers diminished, and the amount of dabs somewhat expanded with expanding dissolving time of the SS/SF blend solution before electrospinning. The amount of dots likewise expanded with expanding SF substance.

The SS/SF (100/0, 75/25, and 50/50) blend nanofibers were effortlessly dissolved in water, while the SS/SF (25/75 and 0/100) blend nanofibers were not totally dis¬solved in water. The SS/SF blend nanofibers were not dissolved in methanol. From the FTIR estimations, the SS/SF blend nanofibers were indicated to own an arbitrary curl compliance and fi-sheet structure. Consistent with FTIR, DSC, and DTA estimations, "as-spun" nanofibers, incorporating SS, SS/SF, and SF nanofibers, held little measures of TFA utilized as the solvent to disintegrate the samples. For the SS/SF (50/50) blend nanofibers hotness treated at 160°c, the TFA held in the specimen nano- fibers was just about totally uprooted.

These SS/SF nanofibers are of impressive investment for various types of provision since these proteins have particular capacities, as specified in the presentation part, and interesting properties incorporating similarly high particular surface range, and so forth.

REFERENCES

Aramwit P., Sangcakul A. (2007). The effects of sericin cream on wound healing in rats. Biosci Biotechnol Biochem, 71: pp. 2473.

Cai Z.X., Mo X.M., Zhang K.H., Fan L.P., Yin A.L., He C., Wang H.S. (2010). Fabrication of chitosan/silk fibroin composite nanofibers for wound-dressing applications. Int J Mol Sci, 11: pp. 3529.

He W., Ma Z.W., Yong T., Teo W.E. (2005). Ramakrishna S: Fabrication of collagen-coated biodegradable polymer nanofiber mesh and its potential for endothelial cells growth. Biomaterials, 26: pp. 7606.

Horan R.L., Antle K., Collette A.L., Wang Y.Z., Huang J., Moreau J.E., Volloch V., Kaplan D.L., Altman G.H. (2005). In vitro degradation of silk fibroin. Biomaterials 2005, 26: pp. 3385.

Huang Z.M., Zhang Y.Z., Kotaki M., Ramakrishna S. (2003). A review on polymer nanofibers by electrospinning and their applications in nanocomposites. Composites Science and Technology, 63: pp. 2223.

Khan M.R., Morikawa H., Gotoh Y., Miura M., Ming Z., Sato Y., Iwasa M. (2008). Structural characteristics and properties of Bombyx mori silk fiber obtained by different artificial forcibly silking speeds. International Journal of Biological Macromolecules, 42: p. 264.

Meinel L., Hofmann S., Karageorgiou V., Head C.K., McCool J., Gronowicz G., Zichner L., Langer R., Novakovic G.V., Kaplan D.L. (2005). The inflammatory responses to silk films in vitro and in vivo. Biomaterials, 26: pp. 147.

Mondal M., Trivedy K., Kumar S.N. (2007). The silk proteins, sericin and fibroin in silkworm, Bombyx mori Linn., - a review. Caspian J Env Sci, 5: p. 63.

Murphy A.R., John P.S., Kaplan D.L. (2008). Modification of silk fibroin using diazonium coupling chemistry and the effects on hMSC proliferation and differentiation. Biomaterials, 29: pp. 2829.

Park WH, Jeong L, Yoo DI, Hudson S. (2004). Effect of chitosan on morphology and conformation of electrospun silk fibroin nanofibers. Polymer, 45: pp. 7151.

Riboldi S.A., Sampaolesi M., Neuenschwander P., Cossu G., Mantero S. (2005). Electrospun degradable polyester-urethane membranes: potential scaffolds for skeletal muscle tissue engineering. Biomaterials, 26: pp. 4606.

Schindler M., Ahmed I., Kamal J., Nur-E-Kamal A., Grafe T.H., Chung H.Y., Meiners S. (2005). A synthetic nanofibrillar matrix promotes in vivo-like organization and morphogenesis for cells in culture. Biomaterials, 26: pp. 5624.

Wharram S.E., Zhang X., Kaplan D.L., McCarthy S.P. (2010). Electrospun silk material systems for wound healing. Macromol Biosci 2010, 10: p. 246.

Zhang Y.Q. (2002). Applications of natural silk protein sericin in biomaterials. Biotechnology Advances, 20: p. 91.

Zong X, Ran SF, Fang D, Hsiao BS, Chu B. (2003). Morphology and property in electrospun poly(glycolide-co-lactide) non-woven membranes via post- draw treatments. Polymer, 44: pp. 4959.

Corresponding Author

Deepti*

Research Scholar, Magadh University, Department of Zoology, A.N. College, Patna

E-Mail – mahesh_gwalior@yahoo.co.in